Parametric Study of Helical Baffle Type Heat Exchanger using 3DEXPERIENCE Platform

Shashank Wankhede, Suryakant Nagdewe, and Kedar Walvekar

3DPLM Software Solutions Limited, Pune-411057, India

Abstract*: Heat exchangers are essential components in many engineering processes in industries. Helical baffle and segmental baffle are two major types of shell and tube heat exchangers. Helical baffle heat exchangers offer lower pressure drops and higher heat transfer efficiency as compared to segmental baffles. In present work, numerical simulations are performed on a helical baffle heat exchanger using 3DEXPERIENCE flow simulation application to predict heat transfer and pressure drop. Since helical baffle inclination angle is an important design parameter, a parametric study is carried out to evaluate its effect on pressure drop and heat transfer. Optimum baffle angle found in the present study is baffle angle of* 35^0 *for which pressure drop and heat transfer is best.*

Keywords*: 3DEXPERIENCE, CFD, Heat Exchanger, Helical Baffle angle, Heat Transfer*

1. Introduction

Heat exchangers play an important role in many engineering processes such as oil refining, chemical industry, electric power generation, refrigeration etc. The shell-and-tube heat exchangers (STHXs) are commonly used because of their robust design as well as easy maintenance. Baffles are used in STHXs to generate local mixing and turbulence in the flow, thereby increasing heat transfer efficiency. Helical and segmental are commonly used types of baffles. Segmental baffles make the fluid flow in a tortuous, zigzag manner across the tube bundle. This improves the heat transfer but has few disadvantages such as high pressure drop, flow stagnation and vibration [3]. The STHXs with helical baffles (STHXHBs), also called as helixchangers offer advantages in terms of improved shell side heat transfer rates/pressure drop ratio, reduced bypass effects, reduced shell-side fouling, prevention of flow induced vibration and reduced maintenance. These advantages of helical baffles have been investigated through experiment and numerical simulations by [2, 4 and 7]. Also the studies have shown the importance of baffle inclination angle on the heat transfer and pressure drop [1, 9 and 8]. It is observed from these studies that with reduction in baffle inclination angle heat transfer increases but it causes higher pressure drop. Present study aims to find out the optimal baffle inclination angle for continuous helical baffle heat exchanger using 3DEXPERIENCE platform. A parametric study is carried out with 15^0, 25^0, 35^0, 45^0 and 55^0 baffle angle. For this study CFD simulations are carried out using flow simulation application.

2. Computational Model and Mesh Generation

The STHXHBs under study [5] is shown in Figure 1 and the geometry parameters are listed in Table 1. Geometric model is built on Part Design with helical baffle angle parameterized. Present STHXHBs has 24 tubes and helical pitch (B) is determined by following equation,

$$B = \pi D_i \tan \beta \quad (1)$$

where β is helix angle and D_i is the inner diameter of shell.

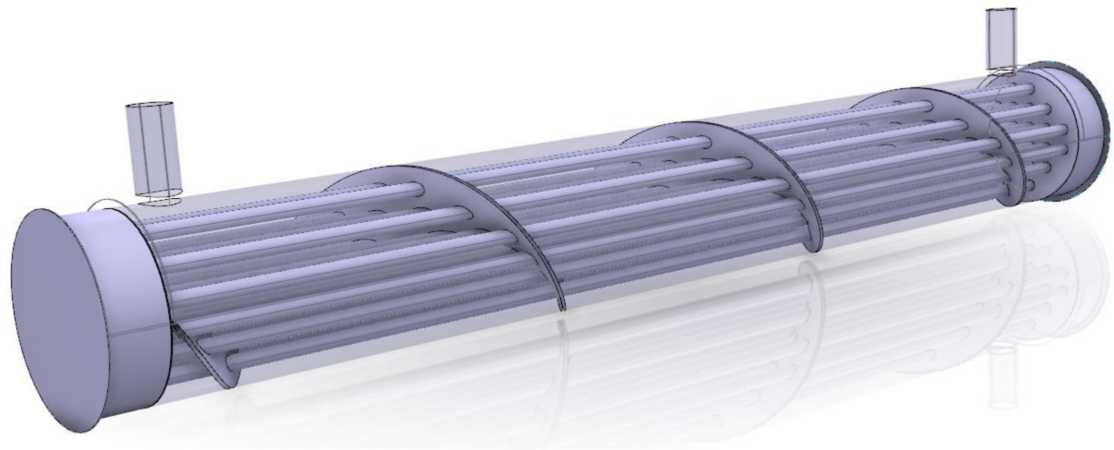

Figure1. STHXHBs model

Table 1: Geometry parameters for the whole STHXHB model

Geometry Notation	Dimensions
Shell Outer Diameter	167mm
Shell Outer Diameter	153mm
Shell Length	1123mm
Tube Inside Diameter	9.5mm
Tube Outside Diameter	12.5mm
No of tube	24
Tube layout	Rectangular
Tube Pitch	22.5
Baffle thickness	4mm
Nozzle Outside Diameter	35mm
Nozzle Inside Diameter	32mm
Head Length	100mm

The whole computational domain is bounded by the inner side of the shell. The inlet and outlet of the domain are connected with the outer shell diameter as shown in Figure 1. CFD mesh is generated using automatic Hex mesher tool. This tool discretizes the computational domain into hex dominant mesh with hexahedral elements (approx. 85%) and other types like tetrahedral, wedge and pyramid. Near wall regions are meshed with boundary layers. Grid independence tests have been carried out for one helical baffle angle 35^0. The calculations were carried out with three different grid densities 1437743, 2775031 and 3018694 elements. It was found that pressure drop and heat transfer results of grid 277,5031and 3018694 are marginally different. Considering both convergent time and solution precision, the grid system of 2775031 is adopted for the computational model. The mesh of the computational domain is shown in Figure 2.

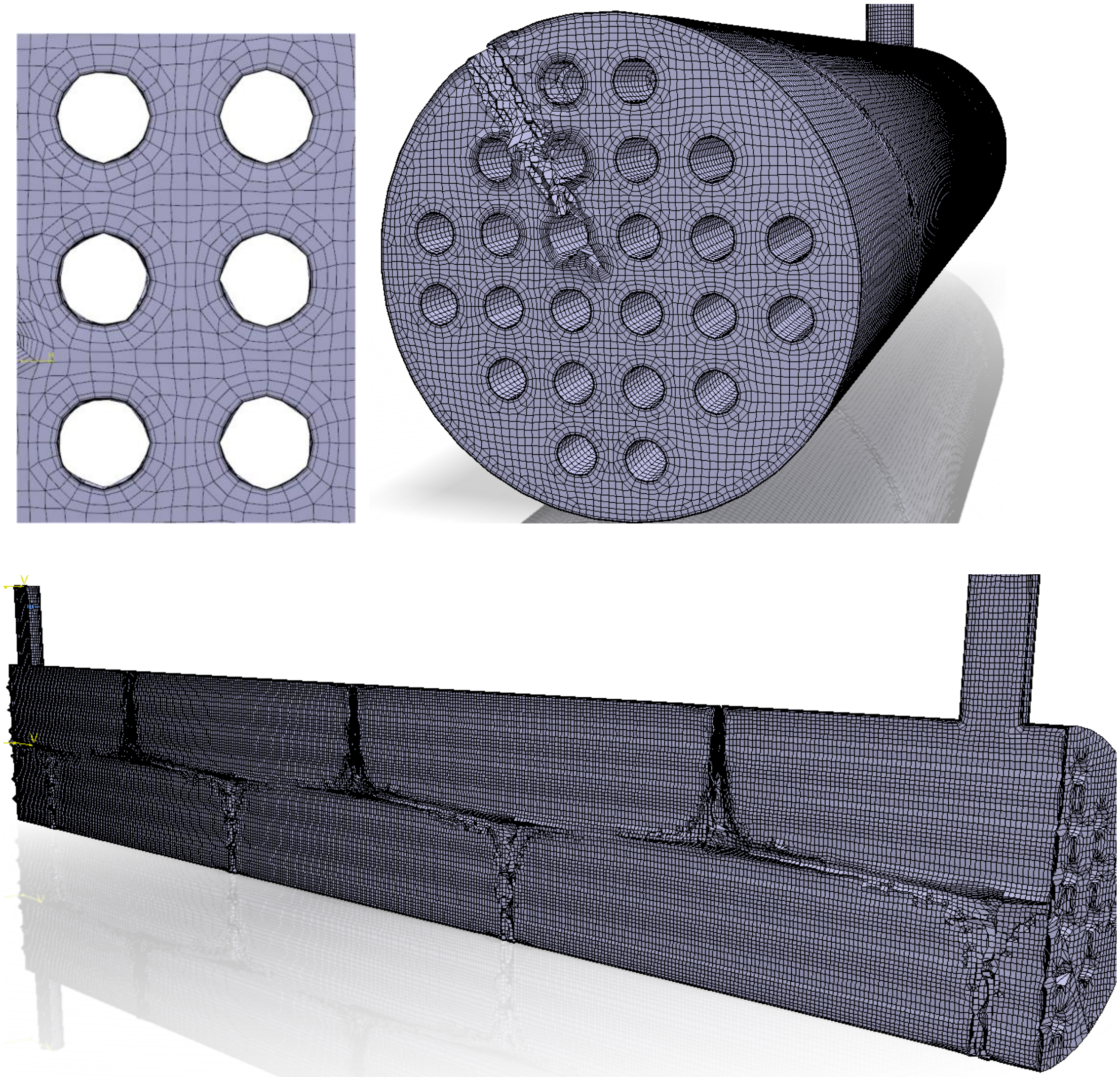

Figure 2. Computational grid with boundary layers

3. Numerical Modeling

3.1 Governing equations

Governing equation for steady state solver is written in integral form of momentum and energy conservation equation as [6],

$$\int_S \rho v \otimes v \cdot n\, dS = -\int_V \nabla p\, dV + \int_S \tau \cdot n\, dS + \int_V f\, dV, \qquad (2)$$

$$\int_S \rho C_p\, \theta\, v \cdot n\, dS = \int_V r\, dV - \int_S q \cdot n\, dS, \tag{3}$$

where V as an arbitrary control volume with surface S, n outward normal to S, ρ is the fluid density, p is the pressure, v is the velocity vector, v_m is the velocity of moving mesh, f is the body force, τ is the viscous shear stress, Cp is the constant pressure specific heat, θ is the temperature, q is heat flux and r is heat supplied externally into the body per unit volume. Here energy Equation 3 is solved in terms of temperature.
Incompressibility condition is specified as,

$$\nabla \cdot v = 0. \tag{4}$$

In present simulation, most popular two-equation k-ε Realizable turbulence model selected. This turbulence model solves an equation of turbulent kinetic energy k and the energy dissipation rate ε. The model equations for k and ε are,

$$\frac{d}{dt}\int_V \rho\, k\, dV + \int_S \rho\, k\left(v - v_m\right)\cdot n\, dS = \int_S (\mu + \frac{\mu_T}{\sigma_k})\, \nabla k \cdot n\, dS + \int_V \left(\tau_{ij}\, S_{ij} + G_b\right) dV - \int_V \rho\, \varepsilon\, dV, \tag{5}$$

$$\frac{d}{dt}\int_V \rho\, \varepsilon\, dV + \int_S \rho\, \varepsilon\left(v - v_m\right)\cdot n\, dS = \int_S (\mu + \frac{\mu_T}{\sigma_\varepsilon})\, \nabla \varepsilon \cdot n\, dS + \int_V C_{\varepsilon 1} (\rho S_\varepsilon + \frac{\varepsilon}{k} C_{\varepsilon 3} G_b)\, dV$$
$$- \int_V C_{\varepsilon 2} \frac{\rho \varepsilon^2}{(k + \sqrt{\upsilon \varepsilon})} dV, \tag{6}$$

where, the Reynolds stress tensor is defined as,

$$\tau = 2 \mu_T S_{ij} \tag{7}$$

With eddy viscosity μ_T is defined as

$$\mu_T = C_\mu \frac{\rho k^2}{\varepsilon} \tag{8}$$

Please refer user manual [6] for turbulence model constant and numerical implementation in details.

Steady state solver solution approach is based on a SIMPLE algorithm on a fixed mesh. A node-centered finite-element discretization for the pressure and a cell-centered finite volume discretization of all the other transported variables are adopted. This hybrid approach guarantees accurate solutions and eliminates the possibility of spurious pressure modes while retaining the local conservation properties associated with traditional finite volume methods. An edge-based implementation is used for all transport equations. In order to increase the accuracy of the k-ε Realizable model in cases where the mesh is not fine enough to resolve the inner layer in wall-bounded flows, a near-wall model, known as two-layer, is implemented to increase the accuracy of the predictions.

3.2 CFD simulation using flow simulation application

No-slip boundary condition is applied on the inner walls of the STHXHBs and all solid surfaces within the computational domain. Velocity inlet and pressure outflow boundary conditions are applied on the inlet and outlet sections respectively. The temperature of tube walls are set as constant and their values are taken from the average wall temperature determined in the experiments [5]. The inner wall of STHXHBs is set as adiabatic. Water is considered as working fluid with properties not varying with temperature.

Following assumptions are made:

- Fluid flow and heat transfer processes are turbulent and in steady-state
- Natural convection induced by the fluid density variation is neglected
- Tube wall temperatures are kept constant in the whole shell side
- Heat exchanger is well-insulated hence the heat loss to the environment is totally neglected.

Inflow conditions are modeled as mass flow rate of 0.84 Kg/s and temperature of 301 K. A constant tube wall temperature of 338 K is considered. Steady state solver with *k-ε* Realizable turbulence model and energy equation is solved. Under-relaxation factor for momentum, turbulence, energy and pressure equation selected are 0.8, 0.8, 0.9 and 0.2 respectively. DSFGMRES solver used to solve momentum, turbulence and energy equations and AMG solver for pressure equation. Residual convergence plot of 25^0 simulations is shown in Fig 3. It is seen from Fig 3 that solution has converged at 1500 iterations.

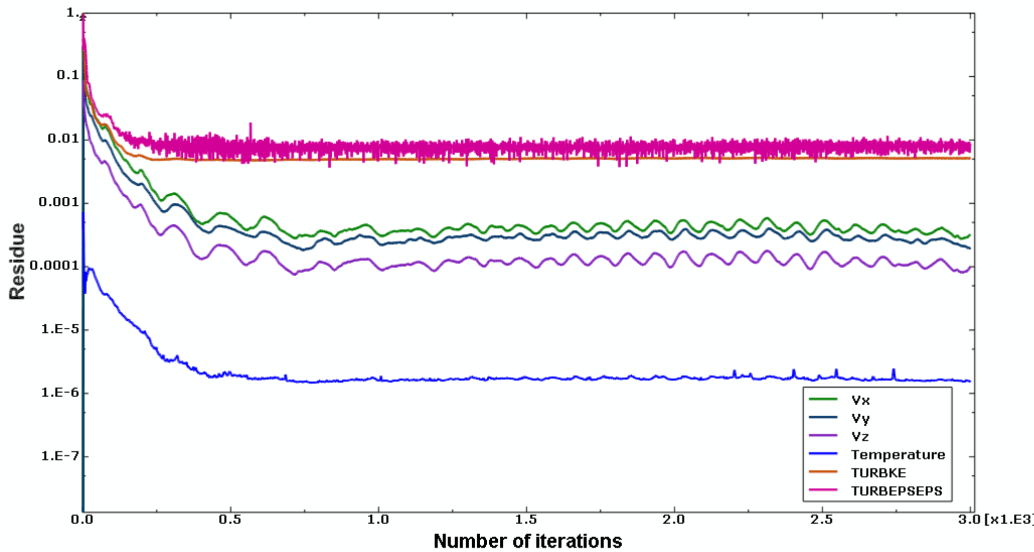

Figure 3. Residual convergence plot.

4. Results and Discussion

Figure 4, 5, 6 and 7 shows streamline plot, velocity vector plot, pressure and temperature distribution respectively. The following observations are made from these analyses,

- The baffles form a helical path for flow thereby avoiding abrupt change in direction of flow. This helps in removing stagnation region and reduces pressure drop
- The absence of back flow or vortex in flow increases heat transfer
- The helical motion brings better mixing which results in significantly enhanced heat transfer.

- Velocity gradient near tube walls indicate that the tube walls are washed out by flow stream

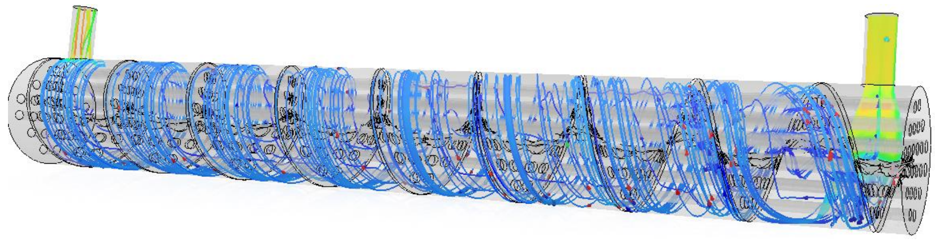

(a)

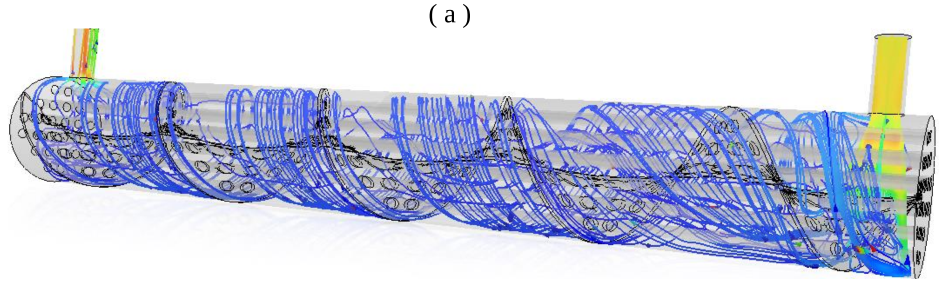

(b)

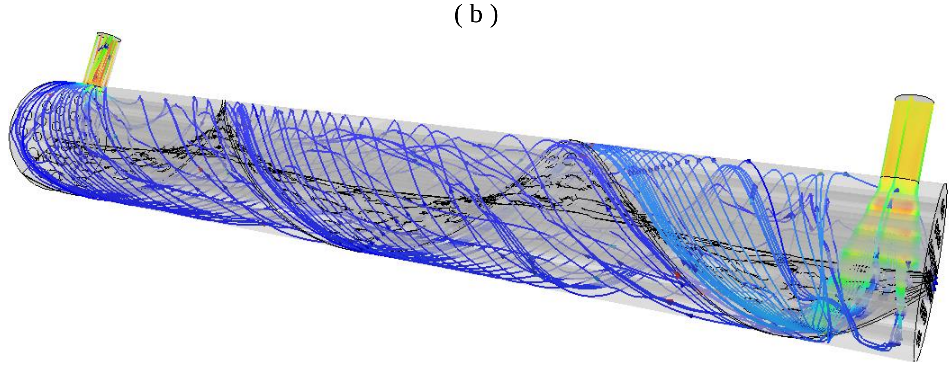

(c)

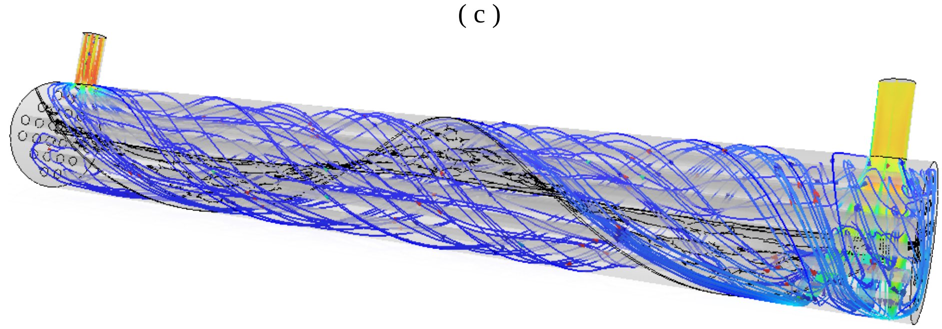

(d)

Figure 4. Stream lines in the shell side for different baffle angles (a) 15^0 and (b) 25^0 (c) 45^0 and (d) 55^0

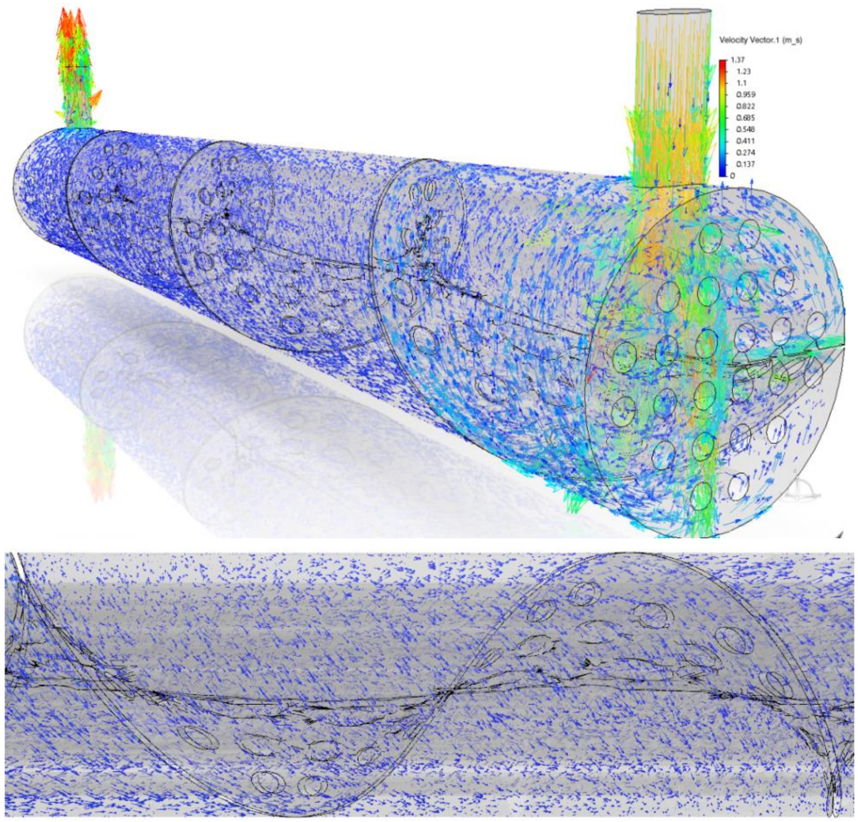

Figure 5. Velocity vectors plot for baffle angle 35^0

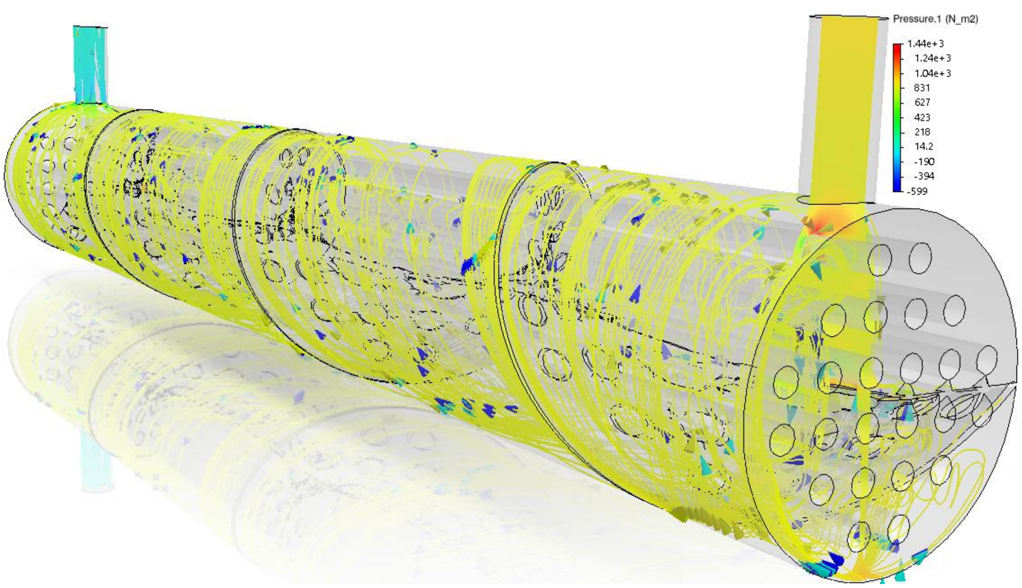

Figure 6. Pressure plot with stream lines for baffle angle 35^0

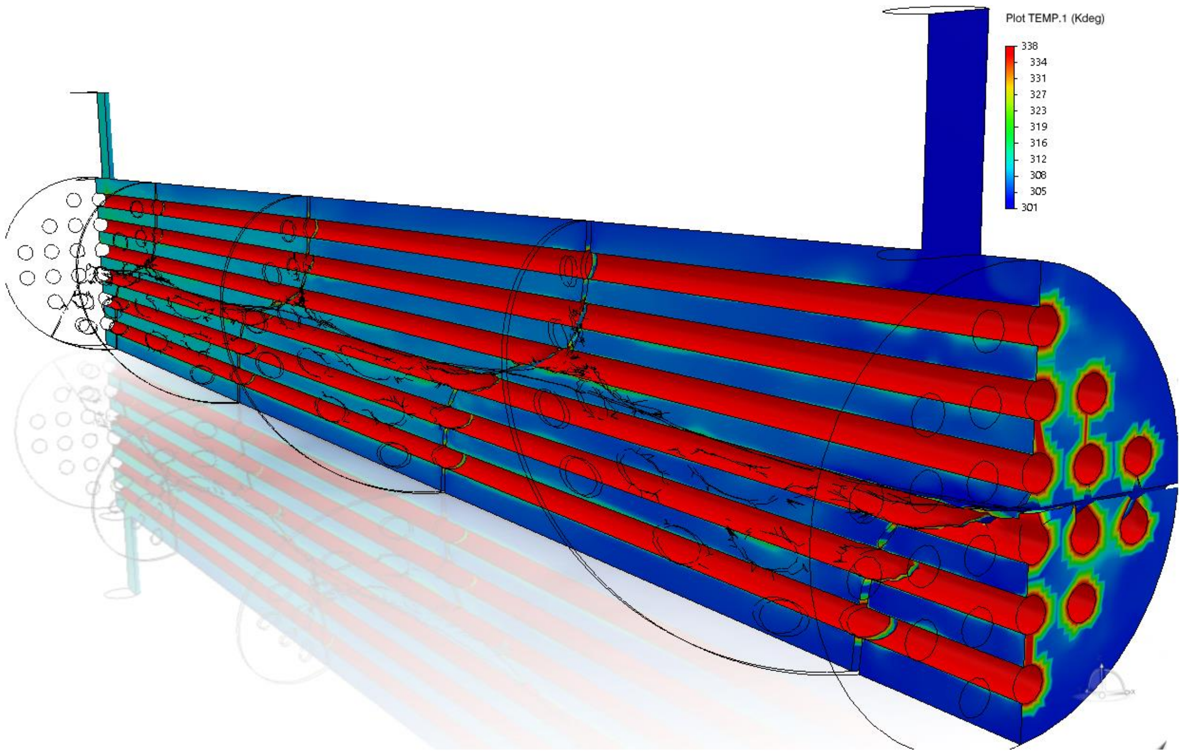

Figure 7. Temperature distributions over the STHXHBs for baffle angles 35^{0}.

Figure 8 and 9 shows the results of parametric study for pressure drop and temperature difference. It is observed that higher pressure drop of 358 N/M^{2} is at baffle angle 15^{0}, as the baffle angle increases, pressure drop reduces. For the baffle angle 35^{0} and 45^{0}, not much change in pressure drop observed. Temperature difference between inlet and outlet sections as an indicator of the amount of heat transferred to the fluid. Higher value of temperature difference indicates higher efficiency of heat exchanger. As the baffle angle increases, temperature difference decreases. It is concluded that baffle angle 35^{0} show moderate heat transfer and low pressure drop.

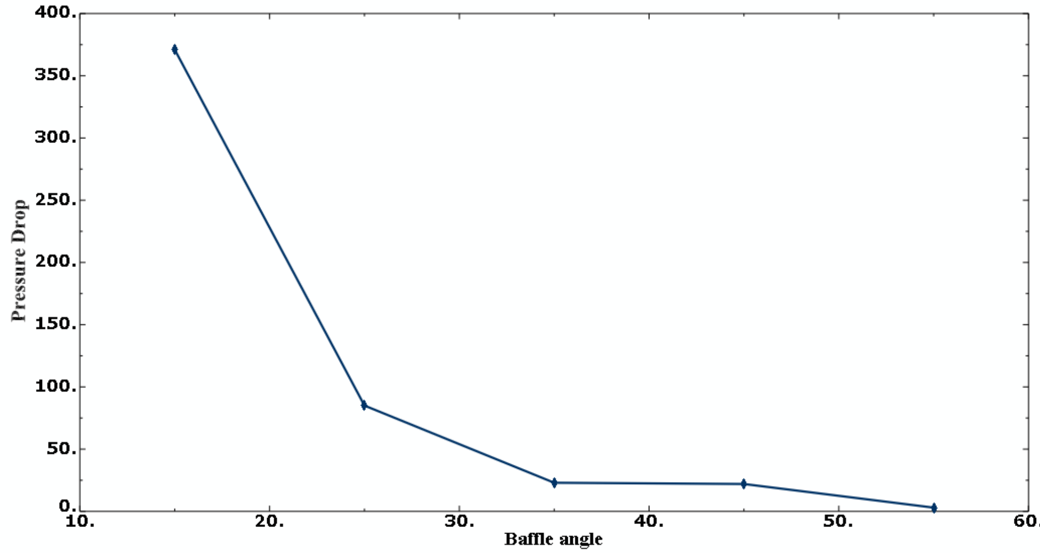

Figure 8. Pressure drop for different baffle angle

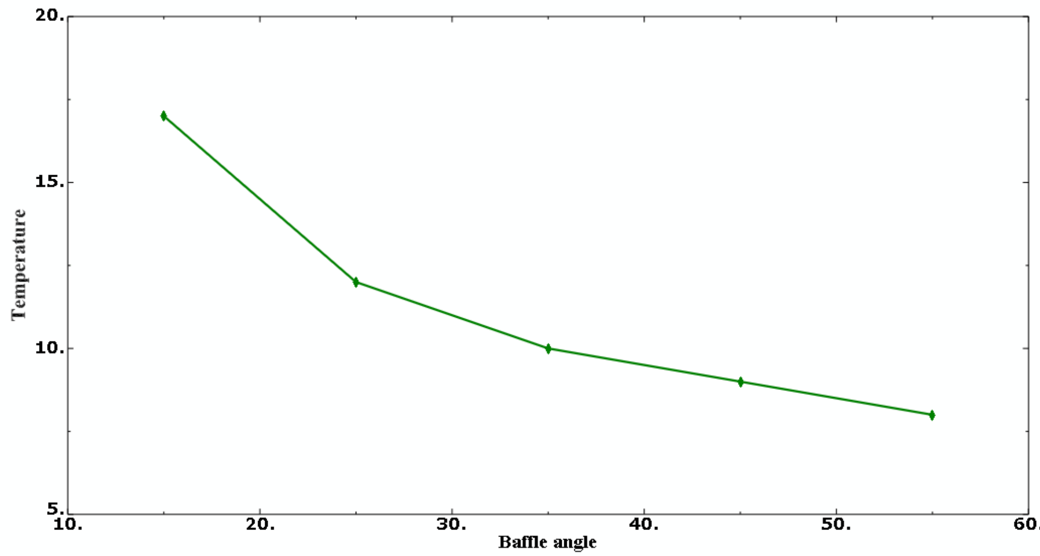

Figure 9. Temperature difference at inlet and outlet of STHXHBs for different baffle angle

5. Conclusion

In present work, numerical simulations are performed on a helical baffle heat exchanger using 3DEXPERIENCE flow simulation application to predict heat transfer and pressure drop. A parametric study is carried out to evaluate the effect of baffle angle on pressure drop and heat transfer. It is observed that the pressure drop varies drastically with baffle angle and shell-side Reynolds number. The variation of the pressure drop is relatively large for small inclination angle.

Heat transfer from hot tube walls to shell side fluid decrease as baffle angle increase. Present numerical study has shown that helical baffle angle 35^0 show moderate heat transfer and low pressure drop.

6. References

1. Lei, Y.G., He, Y.L., Li, R. and Gao, Y.F., "Effect of baffle inclination angle on flow and heat transfer of a heat exchanger with helical baffles", Chemical Engineering and Processing, 47, 2008, pp. 2336-2345.
2. Peng, B., Wang, Q. W., Zhang, C., Xie, G. N., Luo, L. Q., Chen, Q. Y. and Zeng, M., "An experimental study of Shell-and-Tube heat exchangers with continuous helical baffles", Journal of Heat Transfer, 129, 2007, pp. 1425-1431.
3. Stehlik, P. and Wadekar, V. V., "Different strategies to improve industrial heat exchange", Heat Transfer Engineering, 23 (6), 2002, pp. 36-48.
4. Shinde, S. S., Joshi, S. S. and Pavithran, S., "Performance improvement in single phase tubular heat exchanger using continuous helical baffles", International Journal of Engineering Research and Application, 2, 2012, pp. 1141-1149.
5. Shinde, S. and Pancha, M. H., "Comparative Thermal Performance Analysis of Segmental Baffle Heat Exchanger with Continuous Helical baffle Heat Exchanger using Kern Method", International Journal of Engineering Research and Application , 2 2012, pp. 2264-2271.
6. User Manual - Contents and Simulation Apps
7. Zhang, L., Xia, Y., Jiang B., Xiao, X. and Yang, X., "Pilot experimental study on shell and tube heat exchangers with small-angles helical baffles", Chemical Engineering and Processing, 69, 2013, pp. 112-118.
8. Xiao, X., Zhang, L., Li, X., Jiang, B., Yang, X. and Xia, Y., "Numerical investigation of helical baffles heat exchanger with different Prandtl number fluids", International Journal of Heat and Mass Transfer, 63, 2013, pp. 434-444.
9. Zhang, J. F., He, Y. L. and Tao, W. Q., "3D numerical simulation on shell-and-tube heat exchangers with middle-overlapped helical baffles and continuous baffles – Part II: simulation results of periodic model and comparison between continuous and noncontinuous helical baffles, International Journal of Heat and Mass Transfer, 52, 2009, pp.5381-5389